



Cite this: *Chem. Sci.*, 2020, **11**, 7479

All publication charges for this article have been paid for by the Royal Society of Chemistry

## Molecular crowding effects on the biochemical properties of amyloid $\beta$ -heme, $\text{A}\beta\text{-Cu}$ and $\text{A}\beta\text{-heme-Cu}$ complexes†

Meng Li, <sup>ab</sup> Zhenqi Liu, <sup>ac</sup> Jinsong Ren, <sup>ac</sup> and Xiaogang Qu, <sup>\*ac</sup>

Heme as a cofactor has been proposed to bind with  $\beta$ -amyloid peptide ( $\text{A}\beta$ ) and the formed  $\text{A}\beta\text{-heme}$  complex exhibits enhanced peroxidase-like activity. So far, *in vitro* studies on the interactions between heme, Cu and  $\text{A}\beta$  have been exclusively performed in dilute solution. However, the intracellular environment is highly crowded with biomolecules. Therefore, exploring how  $\text{A}\beta\text{-heme-Cu}$  complexes behave under molecular crowding conditions is critical for understanding the mechanism of  $\text{A}\beta$  neurotoxicity *in vivo*. Herein, we selected PEG-200 as a crowding agent to mimic the crowded cytoplasmic environment for addressing the contributions of crowded physiological environments to the biochemical properties of  $\text{A}\beta\text{-heme}$ ,  $\text{A}\beta\text{-Cu}$  and  $\text{A}\beta\text{-heme-Cu}$  complexes. Surprisingly, experimental studies and theoretical calculations revealed that molecular crowding weakened the stabilization of the  $\text{A}\beta\text{-heme}$  complex and decreased its peroxidase activity. Our data attributed this consequence to the decreased binding affinity of heme to  $\text{A}\beta$  as a result of the alterations in water activity and  $\text{A}\beta$  conformation. Our findings highlight the significance of hydration effects on the interaction of  $\text{A}\beta\text{-heme}$  and  $\text{A}\beta\text{-Cu}$  and their peroxidase activities. Molecular crowding inside cells may potentially impose a positive effect on  $\text{A}\beta\text{-Cu}$  but a negative effect on the interaction of  $\text{A}\beta$  with heme. This indicates that  $\text{A}\beta40\text{-Cu}$  but not  $\text{A}\beta40\text{-heme}$  may play more important roles in the oxidative damage in the etiology of AD. Therefore, this work provides a new clue for understanding the oxidative damage occurring in AD.

Received 20th February 2020  
Accepted 2nd July 2020

DOI: 10.1039/d0sc01020k  
[rsc.li/chemical-science](http://rsc.li/chemical-science)

## Introduction

Alzheimer's disease (AD) is a devastating neurodegenerative disease.<sup>1</sup> One of the important pathological features of AD is the formation of senile plaques, which is caused by the aggregation and cerebral deposition of amyloid  $\beta$ -peptide ( $\text{A}\beta$ ). Targeting, preventing and even reversing aggregation of  $\text{A}\beta$  have been considered to be effective strategies for AD therapy.<sup>2–5</sup> Although promising, till now, there is no known cure for AD, due to the complex pathogenesis of AD.<sup>6–8</sup>

Numerous studies indicate that heme plays a critical role in the neurotoxicity of  $\text{A}\beta$ , which can bind with  $\text{A}\beta$  to form an  $\text{A}\beta\text{-heme}$  complex with enhanced peroxidase-like activity.<sup>7–9</sup> The complex can catalyze the oxidation of neurotransmitters by  $\text{H}_2\text{O}_2$  and induce an abnormality of heme metabolism, leading to enhanced neural damage.<sup>7,9</sup> Moreover, metal ions as cofactors are

also involved in  $\text{A}\beta$  aggregate deposition and neurotoxicity. It has been reported that  $\text{Cu}^{2+}$  accumulated in amyloid plaques is capable of exacerbating the progression of amyloid pathology in AD.<sup>10–12</sup> On the other hand, upon binding to  $\text{A}\beta$ , the formed  $\text{A}\beta\text{-metal}$  complexes can promote oxygen activation to produce toxic reactive oxygen species (ROS) under physiological conditions.<sup>13–16</sup> The produced ROS then in turn result in enhanced aggregation propensity of  $\text{A}\beta$  especially  $\text{A}\beta$  oligomerization,<sup>17</sup> which is thought to be another contributing factor to  $\text{A}\beta$ -related neuronal dysfunction, cellular apoptosis and further amyloid plaque formation.<sup>17–19</sup> More importantly, it has been reported that the amount of toxic ROS produced by  $\text{A}\beta\text{-heme-Cu}$  is obviously higher than that produced by  $\text{A}\beta\text{-heme}$  or  $\text{A}\beta\text{-Cu}$  complexes in dilute solution,<sup>20</sup> which may significantly increase the cytotoxicity. Critically, due to the distribution of  $\text{A}\beta$  peptides both in the cytoplasm and extracellular spaces in the brain,<sup>20,21</sup>  $\text{A}\beta$  would bind to  $\text{Cu}^{2+}$  and heme simultaneously *in vivo*. Therefore, it is highly appropriate to study the combined effects of heme and Cu on  $\text{A}\beta$ -induced neurotoxicity under physiological conditions.

So far *in vitro* analysis of the interaction of  $\text{A}\beta$  with heme and Cu has been exclusively carried out in dilute solution.<sup>20,21</sup> However, in contrast to the *in vitro* solution environments, the cellular environment where  $\text{A}\beta$  peptides exist is highly crowded since various macromolecules occupy up to 40% of the cytoplasmic volume.<sup>22,23</sup> This so-called macromolecule crowding

<sup>a</sup>Laboratory of Chemical Biology, Division of Biological Inorganic Chemistry, State Key Laboratory of Rare Earth Resource Utilization, Changchun Institute of Applied Chemistry, Chinese Academy of Sciences, Changchun, Jilin 130022, P. R. China. E-mail: [xqu@ciac.ac.cn](mailto:xqu@ciac.ac.cn); Fax: +86-431-85262656

<sup>b</sup>College of Pharmaceutical Sciences, Hebei Medical University, Shijiazhuang, 050017, P. R. China

<sup>c</sup>University of Science and Technology of China, Hefei, Anhui 230026, P. R. China

† Electronic supplementary information (ESI) available. See DOI: [10.1039/d0sc01020k](https://doi.org/10.1039/d0sc01020k)



effect makes the behaviors of peptides in a cellular environment quite different from that in dilute solution. It can accelerate protein aggregation to form a compact state due to the reduced available volume.<sup>24</sup> In addition, as the water activity decreased, the protein solubility was reduced, resulting in the self-assembly of amyloidogenic proteins.<sup>24–26</sup> Given such a profound influence on A $\beta$  aggregation, investigating the effects of molecular crowding on A $\beta$ –heme–Cu interaction is of great significance. In this study, in order to address the contributions of crowded physiological environments to the biochemical properties of the A $\beta$ –heme–Cu complex, we utilized a concentrated solution of PEG-200, one of the commonly used molecular crowding agents, to mimic the crowded cellular environment.<sup>27,28</sup> A $\beta$ 40, the most abundant A $\beta$  isoform, was chosen as the peptide model for this study.

## Materials and methods

### Materials

3,3',5,5'-Tetramethylbenzidine (TMB) was purchased from Damas-beta (Shanghai, China). H<sub>2</sub>O<sub>2</sub> was bought from Beijing Chemicals (Beijing, China). Heme was purchased from Alfa Aesar (Ward Hill, MA). Glycerol, polyethylene glycol with an average molecular weight of 200 (PEG-200) and 1,1,1,3,3,3-hexafluoropropan-2-ol (HFIP) were obtained from Acros Organics. Other chemicals used in this study were purchased from Sigma-Aldrich. All these reagents were used as received without further purification. Deionized water (D.I. water, 18.2 M $\Omega$  cm) used for all experiments was obtained from a Milli-Q system (Millipore, Bedford, MA).

### A $\beta$ preparation

A $\beta$ 40 (lot no. ALX-151-003) was obtained from Enzo Life Sciences and prepared according to previous reports.<sup>29–31</sup> Briefly, the peptide was dissolved in HFIP at a concentration of 2 mg mL<sup>−1</sup> under shaking at 4 °C for 4 hours in a sealed vial for complete dissolution. After that, the peptide was stored at −20 °C. Before experiments, the solvent HFIP was removed by evaporation under a gentle stream of nitrogen and the peptide was dissolved in phosphate buffered saline (PBS, pH 7.0), which was then used immediately.

### Preparation of heme

A stock solution was prepared by dissolving heme in dimethyl sulfoxide (DMSO) and stored at −20 °C. The concentration of heme was determined spectrophotometrically using a millimolar extinction coefficient of 179 at 404 nm in 40% DMSO.<sup>32</sup> The concentration of the stock solution was 32 mM. The heme working solution was freshly prepared with PBS (pH 7.0), which contained 137 mM NaCl, 2.7 mM KCl, 10 mM Na<sub>2</sub>HPO<sub>4</sub>, and 2 mM KH<sub>2</sub>PO<sub>4</sub>. The final concentration of DMSO was kept lower than 0.8% for all assays.

### Preparation of different complexes

A $\beta$ 40–heme was formed by incubating A $\beta$ 40 with heme at a molar ratio of 1 : 1 for 1 h. Similarly, A $\beta$ 40–Cu complex was

prepared *via* incubating CuCl<sub>2</sub> solution with A $\beta$ 40 at a molar ratio of 1 : 1 for 1 h. The incubation of CuCl<sub>2</sub> solution with the preformed A $\beta$ 40–heme at a molar ratio of 1 : 1 (Cu<sup>2+</sup> : A $\beta$ 40) for 1 h can give the A $\beta$ 40–heme–Cu complex, while the sample of A $\beta$ 40–Cu–heme was obtained by incubating heme with the preformed A $\beta$ 40–Cu complex at a molar ratio of 1 : 1 (heme : A $\beta$ 40) for 1 h. All the complexes were prepared in PBS. The final pH value of all the complexes was kept at 7.0.

### Electron paramagnetic resonance (EPR) analysis

EPR spectra were acquired with a Bruker A3000 electron paramagnetic resonance spectrometer. The concentration of EPR samples was 0.25 mM, and the experiments were run at 77 K in a liquid nitrogen finger dewar.

### Fluorescence titrations

Quenching of the intrinsic fluorescence of tyrosine was monitored according to previous reports.<sup>30,31</sup> Different concentrations of heme (0–7  $\mu$ M) were incubated with A $\beta$ 40 (3  $\mu$ M) in various concentrations of glycerol. Then the fluorescence spectra of these samples were collected with the excitation wavelength at 278 nm. The emission intensity at 306 nm was recorded for analysis. To calculate the binding constants, the 1 : 1 binding stoichiometric equation<sup>29,33</sup> was employed:

$$I = I_0 + 0.5 \left( \frac{\Delta I}{[P]} \right) \times \left( [P] + [L] + K_d - \left( ([P] + [L] + K_d)^2 - 4[P][L] \right)^{1/2} \right)$$

where [P] indicates the concentration of A $\beta$ 40 and [L] is the concentration of heme.  $\Delta I$  represents the difference in fluorescence intensities of the free and complexed A $\beta$ 40 peptides. The binding constant:  $K = 1/K_d$ .

The change in hydration is given by the equation:<sup>29,34</sup>

$$(\partial \ln(K_s/K_0)) / \partial [\text{Osm}] = -\Delta n_w / 55.5$$

where  $K_s$  is the binding constant at a given osmolyte concentration and  $K_0$  is the binding constant in dilute solution. “Osm” is the osmolality of the solution.  $\Delta n_w$  is the difference in the number of bound water molecules between the complex and the free reactants.

### Peroxidase activities of the different complexes

TMB was utilized as the substrate for evaluating the catalytic abilities of the different A $\beta$ 40-related complexes. The measurements were performed by monitoring the absorbance change at 652 nm. To perform this assay, 4  $\mu$ L TMB (42 mM), 4  $\mu$ L H<sub>2</sub>O<sub>2</sub> (300 mM) and 4  $\mu$ L of heme or the formed complexes (80  $\mu$ M) were successively added into 388  $\mu$ L PBS (pH 5.0). For the comparison of the different peroxidase activities of these complexes, the absorbance at 652 nm was monitored after 1 h of incubation at 37 °C. Methylene blue (MB) was also utilized to determine the peroxidase activities of these different complexes under neutral pH conditions.<sup>8</sup> A PBS solution (200  $\mu$ L, pH = 7) containing the formed complexes (2  $\mu$ M), H<sub>2</sub>O<sub>2</sub> (1 mM) and MB



(10  $\mu\text{M}$ ) was prepared. After 2 h of incubation at 37 °C, the absorbance change of MB at 664 nm was monitored by using a microplate reader (molecular devices, SpectraMax Plus 384).

### In vitro ROS measurements

The produced ROS by A $\beta$ 40 related complexes in the presence of a reducing agent (ascorbate) was detected using Amplex Red/horseradish peroxidase (HRP) assays.<sup>35</sup> Different A $\beta$ 40 related samples (5  $\mu\text{M}$ ) in PBS (pH 7.0) were first mixed with HRP (1 U  $\text{mL}^{-1}$ ) and Amplex Red (50  $\mu\text{M}$ ). The formation of resorufin was initiated by the addition of ascorbate (50  $\mu\text{M}$ ) in the reaction mixture. The total volume of the sample solution was 400  $\mu\text{L}$ . After incubation for 45 min, the formation of ROS was determined by the measurement of the fluorescence intensity at 590 nm with an excitation wavelength of 540 nm. The interference of PEG-200 on the detection of ROS was eliminated by the measurement of  $\text{H}_2\text{O}_2$  with the given concentrations to obtain a calibration curve in the presence of different concentrations of PEG-200. The amount of ROS produced by these complexes was normalized with that produced by A $\beta$ 40–heme in dilute solution. Each experiment was performed in triplicate.

### CD measurements

A Jasco-J810 spectropolarimeter was employed to analyse the secondary conformation of A $\beta$ 40. A path length of the cell of 0.1 cm was used. And the spectrum was measured over the wavelength range from 200 nm to 260 nm. The concentration of A $\beta$ 40 was 50  $\mu\text{M}$ .

### Simulated calculation on optimization molecular interactions

All simulations were performed using the Gaussian 09 program. The structure of heme was obtained from the RCSB PDB database and optimized at the B3LYP level of theory in combination with the 6-31G(d,p) basis set. The constructions of Heme–arginine, heme–histidine and histidine–heme–arginine were investigated at the B3LYP/6-31G(d,p) level. All calculations had no imaginary frequency, indicating that the systems were stable. The interaction energies were computed including the correction of the basis set superposition error (BSSE) at the same level of theory.

## Results and discussion

To clarify the influence of the crowded environment on the interaction of A $\beta$ 40 with heme, we monitored the changes in UV-vis spectra of heme. Since A $\beta$ 40 bound to heme in a binding stoichiometry of 1 : 1 in dilute solution at neutral pH,<sup>9,20</sup> we also used 1 : 1 as the molar ratio of heme to A $\beta$ 40 in the following experiments. As shown in Fig. 1A, upon addition of A $\beta$ 40 to the heme solution, a red shift of the Soret band from about 375 nm to 404 nm and an increase around 530 nm were observed, which indicated the formation of an A $\beta$ 40–heme complex.<sup>9</sup> It was worth noting that the spectrum of heme in the presence of PEG-200 was different from that of free heme. The free movement and vibration of heme may be limited due to the solution effect, which then resulted in reduced absorbance and broader bands

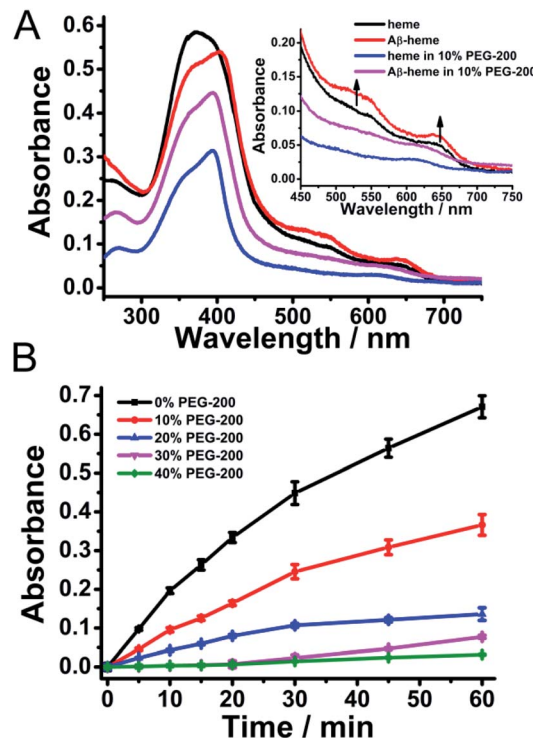


Fig. 1 (A) UV-vis absorption spectra of A $\beta$ 40–heme in the presence of PEG-200. The final concentrations of heme and A $\beta$ 40 were 20  $\mu\text{M}$ , respectively. (B) Peroxidase activity of A $\beta$ 40–heme in the presence of different concentrations of PEG-200. The values were presented as means  $\pm$  SD of three independent experiments.

(Fig. 1A).<sup>36</sup> Under the crowding conditions, the red shift of the Soret band of heme was not induced by A $\beta$ 40 (Fig. 1A). This typical spectral change implied that the binding ability of heme toward A $\beta$ 40 was weakened in the crowding environment.

Given the significantly reduced interaction between heme and A $\beta$ 40 in PEG-200 solution, we then examined the effects of the crowding agent on the peroxidase-like activity of the A $\beta$ 40–heme complex *via* monitoring the catalytic oxidation of TMB by  $\text{H}_2\text{O}_2$ .<sup>37,38</sup> In dilute solution, the catalytic activity of A $\beta$ 40–heme was more than three times higher compared to that of free heme (Fig. S1 and S2, ESI<sup>†</sup>). However, as illustrated in Fig. 1B, the presence of PEG-200 had a dramatic effect on A $\beta$ 40–heme peroxidase activity. The higher the concentration of PEG-200 in the sample, the lower the catalytic activity of A $\beta$ 40–heme. In fact, the catalytic activity of A $\beta$ 40–heme shrunk by about 20 times when the concentration of PEG-200 was up to 40% in PBS (Fig. S2, ESI<sup>†</sup>). As a very modest catalyst under these conditions, the peroxidase activity of A $\beta$ –heme could not be of significance *in vivo*, which was consistent with a previous report.<sup>39</sup> However, in the control experiments, the catalytic activity of heme increased slightly when examined under crowding conditions (Fig. S1 and S2, ESI<sup>†</sup>). Interestingly, in the presence of PEG-200 at a higher concentration, the peroxidase activity of A $\beta$ 40–heme was even lower than that of heme. These results indicated that the weak interactions may not be the only factor that affected the peroxidase activity of the A $\beta$ 40–heme complex under the crowding conditions.



Sequentially, the effect of crowding conditions on the formation of A $\beta$ 40–heme–Cu was examined. As shown in Fig. 2A, upon addition of Cu<sup>2+</sup> to the preformed A $\beta$ 40–heme complex, the characteristic features of A $\beta$ 40–heme were still retained, indicating that the addition of Cu<sup>2+</sup> did not disrupt the preformed A $\beta$ 40–heme complex. Interestingly, if the metal ions were added to A $\beta$ 40 before the addition of heme, there were no characteristic features of A $\beta$ 40–heme (Fig. S3A, ESI<sup>†</sup>), indicating that the bound metal ions were able to inhibit the formation of the A $\beta$ 40–heme complex. These results were consistent with previous studies reported by Atamna,<sup>6</sup> but different from Dey's work.<sup>9</sup> The difference may arise from the different experiment conditions. Meanwhile, similar to the behaviour of A $\beta$ 40–heme under our experimental conditions, the binding affinity of heme with A $\beta$ 40 was too weak to induce the spectral change of heme in A $\beta$ 40–heme–Cu in the presence of PEG-200 (Fig. 2A).

The binding behaviour of Cu<sup>2+</sup> to A $\beta$  was monitored using EPR spectroscopy. As shown in Fig. S4 (ESI<sup>†</sup>), the EPR spectrum of the A $\beta$ 40–Cu complex at pH 7 exhibited a characteristic type 2 Cu<sup>2+</sup> signal in the high field region, with  $g_{\parallel} \sim 2.23$  and  $g_{\perp} \sim 2.053$ . When Cu<sup>2+</sup> was added to the preformed A $\beta$ –heme complex, the high field region of the EPR spectrum of the A $\beta$ –heme–Cu complex was identical to that of the EPR spectrum of

A $\beta$ –Cu. Furthermore, an identical EPR spectrum was also obtained when heme was added to the preformed A $\beta$ –Cu complex. All these results indicated that the formation of A $\beta$ –Cu was unperturbed by the introduction of heme. Critically, the presence of 10% PEG-200 did not change the binding behavior of Cu<sup>2+</sup> to A $\beta$ .

Moreover, the peroxidase activity of the A $\beta$ 40–heme–Cu complex which was measured *via* the oxidation of TMB was comparable with that of the A $\beta$ 40–heme complex in solution (Fig. 2B and S5, ESI<sup>†</sup>). However, under crowding conditions, the peroxidase activity of the A $\beta$ 40–heme–Cu complex was obviously inhibited (Fig. 2B and S5, ESI<sup>†</sup>). It was worth noting that the peroxidase activity of A $\beta$ 40–heme–Cu was higher than that of A $\beta$ 40–heme in the presence of the same concentration of PEG-200 (Fig. S5, ESI<sup>†</sup>), which suggested that the peroxidase activity of A $\beta$ 40–heme–Cu did not just arise from the interaction between A $\beta$ 40 and heme. As a control sample, the A $\beta$ 40–Cu complex showed weak peroxidase activity under the same experimental conditions (Fig. S6, ESI<sup>†</sup>). Interestingly, in the presence of a low concentration of PEG-200, the peroxidase activity of A $\beta$ 40–Cu was slightly enhanced (Fig. S6, ESI<sup>†</sup>), which may be caused by the increased affinity of substrates toward the stable A $\beta$ 40–Cu complex in the presence of a low concentration of the crowding agent.<sup>40,41</sup> Additionally, the peroxidase activity of the heme treated A $\beta$ 40–Cu complex (A $\beta$ 40–Cu–heme) was significantly lower than that of the A $\beta$ 40–heme–Cu complex, further supporting that heme could not bind to A $\beta$ 40 after A $\beta$ 40–Cu complex had formed (Fig. S7, ESI<sup>†</sup>). Critically, to mimic *in vivo* conditions, the peroxidase activities of these A $\beta$ 40 related complexes were also measured at neutral pH. As shown in Fig. S8 (ESI<sup>†</sup>), similar to the finding under acidic conditions, the catalytic activities of A $\beta$ 40–heme, A $\beta$ 40–heme–Cu and A $\beta$ 40–Cu–heme were significantly inhibited in a neutral pH environment under crowding conditions while the catalytic activity of A $\beta$ 40–Cu was slightly enhanced in the presence of a low concentration of PEG-200. That was to say that under crowding conditions, Cu binding to A $\beta$ 40 may play a more critical role in contributing to the peroxidase activity of A $\beta$ 40–heme–Cu.

It has been reported that transition metals and heme can bind to A $\beta$  spontaneously to induce the generation of ROS in dilute solution.<sup>20</sup> And the ROS was generated by the chemical reduction of O<sub>2</sub> by A $\beta$ –Cu<sup>+</sup>, A $\beta$ –heme (Fe<sup>2+</sup>), and A $\beta$ –heme (Fe<sup>2+</sup>)–Cu<sup>+</sup> complexes.<sup>42,43</sup> Both A $\beta$ –Cu and A $\beta$ –heme can react with O<sub>2</sub> in their reduced state, in which O<sub>2</sub> can re-oxidize the reduced Cu<sup>+</sup> site to the Cu<sup>2+</sup> form and the reduced heme site (Fe<sup>2+</sup>) to the Fe<sup>3+</sup> form, respectively, leading to the formation of ROS. In dilute solution, since both the heme and Cu were bound to A $\beta$ , the amount of ROS generated by A $\beta$ –heme–Cu was much more than the individual binder. However, under macromolecular crowding conditions, the binding affinities of Cu and heme with A $\beta$  changed, which would remarkably impact the electron transfer thus affecting the production of ROS. As shown in Fig. 3, upon introduction of PEG-200, the amount of ROS generated by A $\beta$ 40–Cu<sup>+</sup> was increased to some extent, while the levels of ROS associated with A $\beta$ 40–heme (Fe<sup>2+</sup>)–Cu<sup>+</sup> and A $\beta$ 40–heme (Fe<sup>2+</sup>) decreased especially in the presence of higher concentrations of PEG-200. The reduced ROS production and

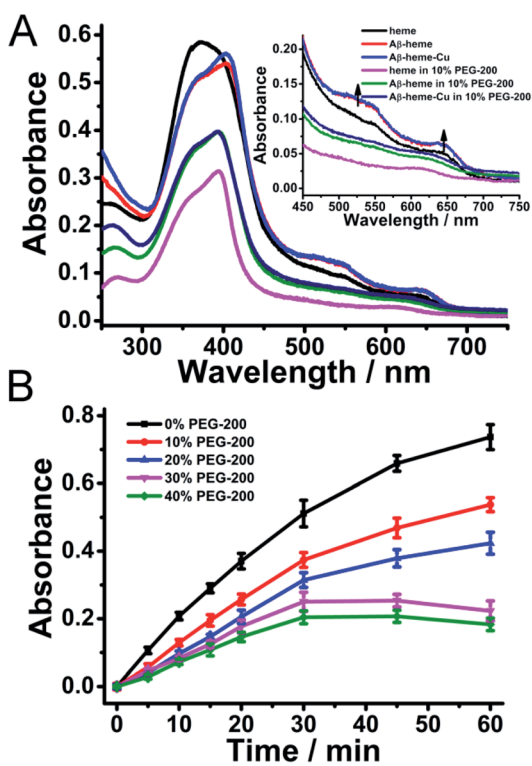


Fig. 2 (A) UV-vis absorption spectra of A $\beta$ 40–heme–Cu in the presence of PEG-200. The concentrations of heme, A $\beta$ 40 and Cu were 20  $\mu$ M. (B) Peroxidase activity of A $\beta$ 40–heme–Cu in the presence of different concentrations of PEG-200. The metal ions were added to A $\beta$ 40 simultaneously with the addition of heme or after the A $\beta$ 40–heme was formed. The values were presented as means  $\pm$  SD of three independent experiments.



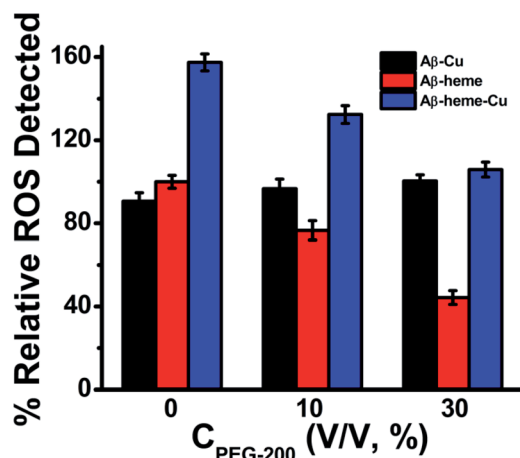


Fig. 3 Amount of ROS detected for the samples of A<sub>β</sub>40–Cu, A<sub>β</sub>40–heme, and A<sub>β</sub>40–heme–Cu with ascorbate by a HRP/Amplex Red assay in the presence of different concentrations of PEG-200. The values were presented as means  $\pm$  SD of three independent experiments.

peroxidase activity of A<sub>β</sub>40–heme ( $\text{Fe}^{2+}$ )–Cu<sup>+</sup> were most attributed to the weak interaction between heme and A<sub>β</sub>40 under macromolecular crowding conditions. That was to say that the harmful ROS generated by these A<sub>β</sub>40 related complexes *in vivo* may be predominantly caused by A<sub>β</sub>40–Cu<sup>+</sup> rather than A<sub>β</sub>40–heme ( $\text{Fe}^{2+}$ ). Therefore, A<sub>β</sub>40–Cu but not A<sub>β</sub>40–heme may play more important roles in the oxidative damage in the etiology of AD, which provided a new clue for understanding the oxidative damage occurring in AD.

As we reported previously,<sup>29</sup> when Cu<sup>2+</sup> binds to A<sub>β</sub>, dehydration occurred, which was accompanied by the release of water from the system. The apparent binding constants of Cu<sup>2+</sup> with A<sub>β</sub> were significantly increased in a crowding environment, where the water activity was perturbed, leading to more stable A<sub>β</sub>–Cu<sup>2+</sup> aggregates,<sup>29</sup> which may facilitate the peroxidase activity of the A<sub>β</sub>–Cu<sup>2+</sup> complex and enhance the amount of ROS produced by A<sub>β</sub>–Cu<sup>+</sup> under macromolecular crowding conditions, while the reduced stabilization of the A<sub>β</sub>–heme complex decreased the generation of ROS associated with A<sub>β</sub>–heme ( $\text{Fe}^{2+}$ )–Cu<sup>+</sup> and A<sub>β</sub>–heme ( $\text{Fe}^{2+}$ ).

To illustrate the mechanism responsible for the reduced stabilization of the A<sub>β</sub>40–heme complex under molecular crowding conditions, we performed spectroscopic titration to analyze the interaction between heme and A<sub>β</sub>40 peptide with or without PEG-200. The binding constants for heme at different concentrations of PEG-200 (from 0–30%) which were determined by using nonlinear least-squares fit of the data from fluorescence titrations were  $3.9 \times 10^5 \text{ M}^{-1}$ ,  $2.6 \times 10^5 \text{ M}^{-1}$ ,  $2.0 \times 10^5 \text{ M}^{-1}$  and  $1.2 \times 10^5 \text{ M}^{-1}$ , respectively (Fig. S9, ESI<sup>†</sup>). This reduced binding affinity well explained the decreased stabilization of the complex and suppressed peroxidase activity in PEG solution.

Furthermore, it has been widely reported that His13 and His14 residues in the A<sub>β</sub> peptide can both bind with heme on the proximal side.<sup>9</sup> After the A<sub>β</sub>–heme complex was formed, the Arg5 residue on the distal side of A<sub>β</sub> can form a H-bond with the

axial water ligand, which then facilitates the O–O bond cleavage, hence making the A<sub>β</sub>–heme complex a peroxidase.<sup>9</sup> The water molecule plays a critical role in mediating the catalytic activity of A<sub>β</sub>–heme. However, molecular crowding can alter the water activity, leading to a hydration change.<sup>27,28</sup> In order to show the roles of water molecules in the activity of A<sub>β</sub>40–heme and how hydration changes occurred upon heme binding to A<sub>β</sub>40, we modulated the water activity of the solution in the presence of an osmotic agent, glycerol. In the absence of osmolyte, the apparent binding constants were  $3.9 \times 10^5$  for heme. Intriguingly, the apparent A<sub>β</sub>40 binding constants for heme were significantly decreased (Fig. 4A) in the presence of glycerol that perturbed the water activity, which were consistent with the behaviours in PEG-200. The apparent binding constants for heme binding to A<sub>β</sub>40 in the presence of glycerol at several different osmolalities were measured. As indicated in Fig. 4B, the apparent binding constants decreased with the increasing concentration of the osmolyte, showing that decreasing water activity weakened the binding of heme to A<sub>β</sub>40.

The dependence of the equilibrium constant on water activity, as determined by osmotic pressure measurements at 25 °C, is shown in Fig. 4B. From the slopes of the least-squares lines, the amount of water involved in the heme–A<sub>β</sub>40

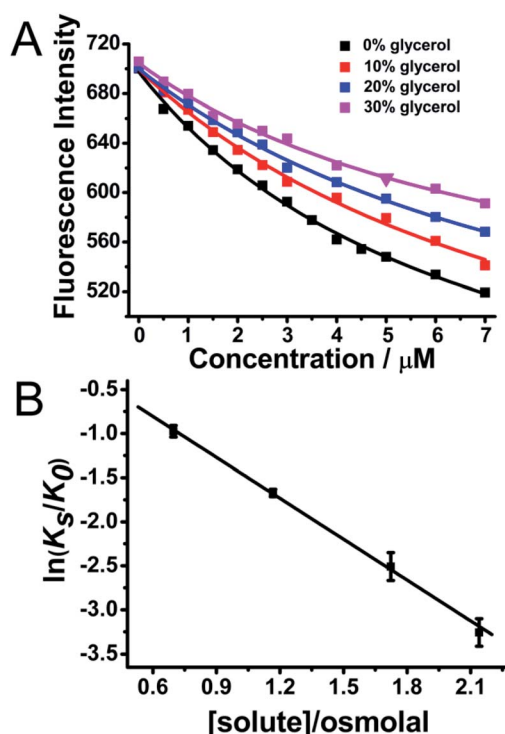


Fig. 4 (A) Fluorescence titration of A<sub>β</sub>40 (3  $\mu\text{M}$ ) with various concentrations of heme at different concentrations of glycerol. The excitation wavelength was 278 nm and the emission intensity at 306 nm was used for analysis. 1 : 1 binding model was used to fit the fluorescence titration data. (B) Relationship between the binding constant and the osmolyte concentration.  $\ln(K_s/K_0)$  the change in binding free energy was plotted against solution osmolality. The values were presented as means  $\pm$  SD of three independent experiments.

**Table 1** Summary of heme binding free energy change and hydration contribution to the binding at 25 °C

A $\beta$ -heme complex	$\Delta G_b^a$ [kcal mol $^{-1}$ ]	$\Delta n_w$	$T\Delta S_{\text{hydration}}^b$ [kcal mol $^{-1}$ ]
A $\beta$ -heme	−7.35	87 ± 3	35.25 ± 10.85

<sup>a</sup>  $G_b = -RT \ln K$ . <sup>b</sup>  $S_{\text{hydration}} = 1.3 \pm 0.4 \text{ cal K}^{-1} \text{ mol}^{-1}$  (the average difference between the partial molar entropy of water in the bulk state and water in the hydration shells of amino acid residues)  $\times n_w$  at 298 K.

interaction can be quantified. The negative slopes of the best-fit lines illustrated that  $\Delta n_w$  was positive with a value of  $87 \pm 3$ , indicating that a substantial number of water molecules were required upon heme binding to A $\beta$ 40. Reducing the number of free water molecules in bulk solution was unfavourable for the complex formation. Furthermore, hydration contribution to the thermodynamics of heme binding processes was also quantified.  $\Delta S_{\text{hydration}}$ , the entropy change caused by the binding-induced change in the hydration of heme and A $\beta$ 40, was calculated<sup>44,45</sup> by using the following equation:  $\Delta S_{\text{hydration}} = 1.3 \pm 0.4 \text{ cal K}^{-1} \text{ mol}^{-1} \times \Delta n_w$ , where  $1.3 \pm 0.4 \text{ cal K}^{-1} \text{ mol}^{-1}$  corresponded to the average difference between the partial molar entropy of water in the bulk state and that of water in the hydration shell of amino acid residues at 298 K, and  $\Delta n_w$  was the number of water molecules required from the bulk state upon the binding of heme to A $\beta$ 40. The value of  $\Delta S_{\text{hydration}}$  was estimated to be  $113.4 \pm 36.4 \text{ cal K}^{-1} \text{ mol}^{-1}$  for heme binding, which was in agreement with a previous report.<sup>39</sup> The contribution of hydration entropy to the binding free energy,  $T\Delta S_{\text{hydration}}$ , was  $35.25 \pm 10.85 \text{ kcal mol}^{-1}$  (Table 1). The value was five fold larger than the net heme–A $\beta$ 40 binding free energy change,  $\Delta G_b = -7.35 \text{ kcal mol}^{-1}$ , showing that hydration was very important in controlling heme binding to A $\beta$ 40.

To further understand the water activity in the interaction of A $\beta$ 40 with heme, the molecular interactions between histidine, arginine and heme in the presence or absence of water were investigated using MD simulations.<sup>46,47</sup> As shown in Fig. 5, without water, histidine could bind with heme on the proximal side; meanwhile, the arginine could just form a weak Fe–O bond with the iron center in heme. The introduction of water molecules totally changed the binding behavior of arginine. The guanidinium side chain of arginine provided H-bonds with the axial water ligand bound to the heme iron center, which was in accordance with a previous report.<sup>9</sup> This binding behaviour also induced a pull effect by providing a proton required to drive the heterolytic cleavage of the O–O bond, resulting in an enhanced peroxidase-like activity of the A $\beta$ –heme complex in the presence of water. The interaction energy obtained by *ab initio* calculations ( $E_{\text{int}}$ ) is summarized in Table S1.<sup>†</sup> The interaction of histidine and arginine with heme in the absence of water was weaker than that in the presence of water, which further supported that hydration was very important in controlling heme binding to A $\beta$ 40.

The interactions of heme and Cu with A $\beta$  were also affected by other factors including the structure of A $\beta$ . A large body of research has found that the nucleation step of amyloidogenic

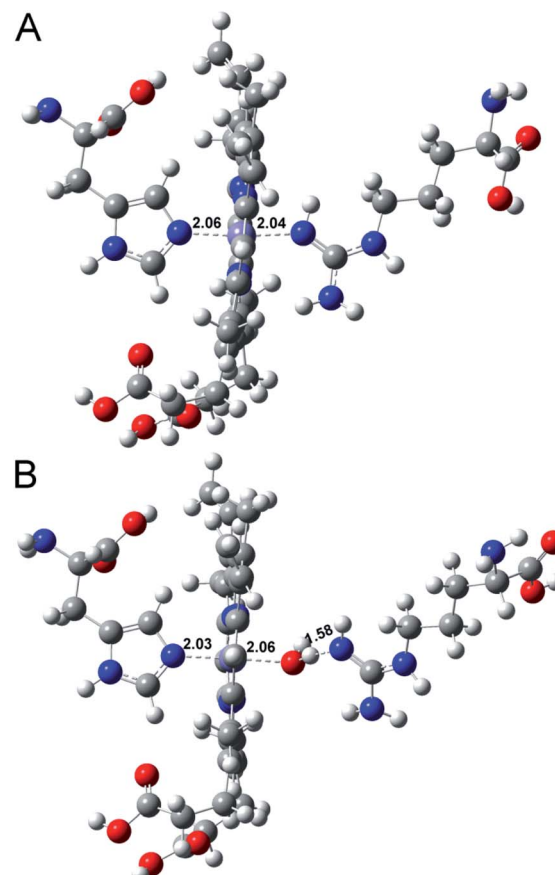
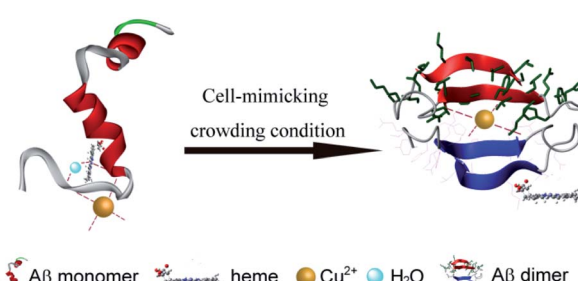


Fig. 5 Energy-minimized average interaction models of Arg–heme–His (A) without water or (B) with water. These complexes were shown in a ball-and-stick model. Carbon atoms are indicated in dark gray balls, hydrogen atoms are in light gray, oxygen atoms are in red, and blue balls define nitrogen atoms. Binding bonds are shown by black dashes.

protein fibrilization can be accelerated in the crowded environment of PEG.<sup>24,48</sup> In accordance with these findings, circular dichroism (CD) spectral analyses (Fig. S10, ESI<sup>†</sup>) clearly showed that the presence of PEG dramatically promoted amyloid fibril formation of A $\beta$ 40. The formed intramolecular or intermolecular  $\beta$ -sheet structure may affect the coordination interaction between heme, Cu and histidine. It has been proposed that A $\beta$ 40 aggregates can also bind a full stoichiometric



**Scheme 1** Schematic representation of the interactions of A $\beta$ , Cu $^{2+}$  and heme under molecular crowding conditions.



complement of Cu<sup>2+</sup> with the same coordination geometry as A $\beta$ 40 monomers, resulting in no changes in their secondary structure.<sup>49,50</sup> Moreover, A $\beta$  fibrils were currently reported to be formed by in-register stacking of A $\beta$  monomers,<sup>49,50</sup> which made the histidine residues at positions 13 and 14 on the A $\beta$  peptide to stack close together in successive peptides to provide a possible Cu<sup>2+</sup> coordination site containing four histidine residues. Therefore, the formation of a  $\beta$ -sheet structure under crowding conditions exhibited no effect on Cu binding to A $\beta$ . Furthermore, the linear two-coordinate N<sub>His</sub>-Cu<sup>+</sup>-N<sub>His</sub> structure played a critical role in the reduced Cu<sup>+</sup>-A $\beta$  species induced ROS production.<sup>51,52</sup> At this point, in the presence of PEG-200, the stated A $\beta$  aggregate may favor the formation of the toxic A $\beta$ -Cu<sup>+</sup> complex *via* an intermolecular histidine bridge.<sup>53</sup> On the other hand, for heme, it was preferred to bind with A $\beta$  monomers rather than A $\beta$  aggregates, leading to the inhibition effect for A $\beta$  fibrilization.<sup>7</sup> The formed  $\beta$ -sheet structure would weaken the coordinative interaction of A $\beta$  with heme. These contributions as well as the decrease of water activity could bring additional complexity into the interaction of Cu and heme with A $\beta$  (Scheme 1).

## Conclusions

In summary, heme as a cofactor has been proposed to interact with A $\beta$  and the formed A $\beta$ -heme complex exhibits peroxidase activity. It is emerging as a promising cytopathology in AD. Together with Cu<sup>2+</sup>, heme bound to A $\beta$  may cause an enhanced cytotoxicity. Therefore, it is of significant importance to see whether heme still works well in the crowded cellular environment. Herein, we select PEG-200, a commonly used crowding agent, to mimic the crowded cellular environment to address the contributions of crowded physiological environments to the biochemical properties of A $\beta$ -Cu, A $\beta$ -heme and A $\beta$ -heme-Cu complexes. Our present study demonstrates that although molecular crowding cannot disturb the binding of Cu with A $\beta$ , it substantially decreases the stabilization of the A $\beta$ -heme complex, inhibits its peroxidase activity and reduces the ROS levels. The reduced stabilization of the A $\beta$ -heme complex arises from the decreased water activity and the altered A $\beta$  conformation. Our findings highlight the significance of the hydration contributions to the interactions of A $\beta$ -heme and A $\beta$ -Cu and their peroxidase activities. The results suggest that A $\beta$ 40-Cu but not A $\beta$ 40-heme may play more important roles in the oxidative damage in the etiology of AD. Therefore, our work provides a new clue for understanding the oxidative damage occurring in AD.

## Conflicts of interest

There are no conflicts to declare.

## Acknowledgements

This work was supported by the National Natural Science Foundation of China (21533008, 21820102009, 91856205, 21807024, and 21871249), Key Program of Frontier of Sciences

(CAS QYZDJ-SSW-SLH052), Youth Top-notch Talents Supporting (BJ2018007) and Hundred Persons Plan of Hebei Province (E2018050012).

## Notes and references

- 1 A. Rauk, *Chem. Soc. Rev.*, 2009, **38**, 2698.
- 2 R. Jakob-Roetne and H. Jacobsen, *Angew. Chem., Int. Ed.*, 2009, **48**, 3030.
- 3 L. E. Scott and C. Orvig, *Chem. Rev.*, 2009, **109**, 4885.
- 4 E. Gaggelli, H. Kozlowski, D. Valensin and G. Valensin, *Chem. Rev.*, 2006, **106**, 1995.
- 5 I. W. Hamley, *Chem. Rev.*, 2012, **112**, 5147.
- 6 H. Atamna and W. H. Frey II, *Proc. Natl. Acad. Sci. U. S. A.*, 2004, **101**, 11153.
- 7 H. Atamna and K. Boyle, *Proc. Natl. Acad. Sci. U. S. A.*, 2006, **103**, 3381.
- 8 C. Yuan, L. Yi, Z. Yang, Q. Deng, Y. Huang, H. Li and Z. Gao, *J. Biol. Inorg. Chem.*, 2012, **17**, 197.
- 9 D. Pramanik and S. G. Dey, *J. Am. Chem. Soc.*, 2011, **133**, 81.
- 10 C. S. Atwood, R. D. Moir, X. D. Huang, R. C. Scarpa, N. M. E. Bacarra, D. M. Romano, M. K. Hartshorn, R. E. Tanzi and A. I. Bush, *J. Biol. Chem.*, 1998, **273**, 12817.
- 11 A. I. Bush, W. H. Pettingell, G. Multhaup, M. D. Paradis, J. P. Vonsattel, J. F. Gusella, K. Beyreuther, C. L. Masters and R. E. Tanzi, *Science*, 1994, **265**, 1464.
- 12 K. P. Kepp, *Chem. Rev.*, 2012, **112**, 5193.
- 13 J. Dong, C. S. Atwood, V. E. Anderson, S. L. Siedlak, M. A. Smith, G. Perry and P. R. Carey, *Biochemistry*, 2003, **42**, 2768.
- 14 L. Guilloréau, S. Combalbert, A. Sournia-Saquet, H. Mazarguil and P. Faller, *ChemBioChem*, 2007, **8**, 1317.
- 15 X. D. Huang, C. S. Atwood, M. A. Hartshorn, G. Multhaup, L. E. Goldstein, R. C. Scarpa, M. P. Cuajungeo, D. N. Gray, J. Lim, R. D. Moir, R. E. Tanzi and A. I. Bush, *Biochemistry*, 1999, **38**, 7609.
- 16 T. Lynch, R. A. Cherny and A. I. Bush, *Exp. Gerontol.*, 2000, **35**, 445.
- 17 C. Guo, L. Sun, X. Chen and D. Zhang, *Neural Regener. Res.*, 2013, **8**, 2003.
- 18 H. Xie, S. Hou, J. Jiang, M. Sekutowicz, J. Kelly and B. J. Bacska, *Proc. Natl. Acad. Sci. U. S. A.*, 2013, **110**, 7904.
- 19 C. M. Lee, S. T. Huang, S. H. Huang, H. W. Lin, H. P. Tsai, J. Y. Wu, C. M. Lin and C. T. Chen, *Nanomedicine*, 2011, **7**, 107.
- 20 D. Pramanik, C. Ghosh and S. G. Dey, *J. Am. Chem. Soc.*, 2011, **133**, 15545.
- 21 D. Pramanik, K. Sengupta, S. Mukherjee, S. G. Dey and A. Dey, *J. Am. Chem. Soc.*, 2012, **134**, 12180.
- 22 S. Muhuri, K. Mimura, D. Miyoshi and N. Sugimoto, *J. Am. Chem. Soc.*, 2009, **131**, 9268.
- 23 L. Stagg, S. Zhang, M. S. Cheung and P. Wittung-Stafshede, *Proc. Natl. Acad. Sci. U. S. A.*, 2007, **104**, 18976.
- 24 L. A. Munishkina, E. M. Cooper, V. N. Uversky and A. L. Fink, *J. Mol. Recognit.*, 2004, **17**, 456.
- 25 L. A. Munishkina, A. Ahmad, A. L. Fink and V. N. Uversky, *Biochemistry*, 2008, **47**, 8993.



26 M. Bokvist and G. Gröbner, *J. Am. Chem. Soc.*, 2007, **129**, 14848.

27 Z. Chen, K. Zheng, Y. Hao and Z. Tan, *J. Am. Chem. Soc.*, 2009, **131**, 10430.

28 S. Nakano, H. Karimata, T. Ohmichi, J. Kawakami and N. Sugimoto, *J. Am. Chem. Soc.*, 2004, **126**, 14330.

29 H. Yu, J. Ren and X. Qu, *ChemBioChem*, 2008, **9**, 879.

30 J. Geng, M. Li, J. Ren, E. Wang and X. Qu, *Angew. Chem., Int. Ed.*, 2011, **50**, 4184.

31 H. Yu, M. Li, G. Liu, J. Geng, J. Wang, J. Ren, C. Zhao and X. Qu, *Chem. Sci.*, 2012, **3**, 3145.

32 K. Kuzelová, M. Mrhalová and Z. Hrkal, *Biochim. Biophys. Acta*, 1997, **1336**, 497.

33 W. Garzon-Rodriguez, A. K. Yatsimirsky and C. G. Glabe, *Bioorg. Med. Chem. Lett.*, 1999, **9**, 2243.

34 X. Qu and J. B. Chaires, *J. Am. Chem. Soc.*, 2001, **123**, 1.

35 X. He, H. M. Park, S. J. Hyung, A. S. DeToma, C. Kim, B. T. Ruotolo and M. H. Lim, *Dalton Trans.*, 2012, **41**, 6558.

36 L. Liu, J. Lin, Y. Song, C. Yang and Z. Zhu, *Chem. Res. Chin. Univ.*, 2020, **36**, 247.

37 Y. Song, K. Qu, C. Zhao, J. Ren and X. Qu, *Adv. Mater.*, 2010, **22**, 2206.

38 M. Mahajan and S. Bhattacharjya, *Angew. Chem., Int. Ed.*, 2013, **52**, 6430.

39 G. Thiabaud, S. Pizzocaro, R. Garcia-Serres, J.-M. Latour, E. Monzani and L. Casella, *Angew. Chem., Int. Ed.*, 2013, **52**, 8041.

40 M. Jiang and Z. Guo, *J. Am. Chem. Soc.*, 2007, **129**, 730.

41 P. Baumann, M. Spulber, O. Fischer, A. Car and W. Meier, *Small*, 2017, **13**, 1603943.

42 C. Ghosh, D. Pramanik, S. Mukherjee, A. Dey and S. G. Dey, *Inorg. Chem.*, 2013, **52**, 362.

43 M. Seal, S. Mukherjee, D. Pramanik, K. Mittra, A. Dey and S. G. Dey, *Chem. Commun.*, 2013, **49**, 1091.

44 G. I. Makhatadze and P. L. Privalov, *Adv. Protein Chem.*, 1995, **47**, 307.

45 D. N. Dubins, R. Filfil, R. B. Macgregor Jr and T. V. Chalikian, *J. Phys. Chem. B*, 2000, **104**, 390.

46 W. Pang, J. Lv, S. Du, J. Wang, J. Wang and Y. Zeng, *Mol. Pharm.*, 2017, **14**, 3013.

47 L. Rodríguez-Santiago, J. Alí-Torres, P. Vidossich and M. Sodupe, *Phys. Chem. Chem. Phys.*, 2015, **17**, 13582.

48 D. Brambilla, R. Verpillot, B. Le Droumaguet, J. Nicolas, M. Taverna, J. Kona, B. Lettiero, S. H. Hashemi, L. De Kimpe, M. Canovi, M. Gobbi, V. Nicolas, W. Scheper, S. M. Moghimi, I. Tvaroska, P. Couvreur and K. Andrieux, *ACS Nano*, 2012, **6**, 5897.

49 C. J. Sarell, C. D. Syme, S. E. J. Rigby and J. H. Viles, *Biochemistry*, 2009, **48**, 4388.

50 A. T. Petkova, Y. Ishii, J. J. Balbach, O. N. Antzutkin, R. D. Leapman, F. Delaglio and R. Tycko, *Proc. Natl. Acad. Sci. U. S. A.*, 2002, **99**, 16742.

51 J. Shearer and V. A. Szalai, *J. Am. Chem. Soc.*, 2008, **130**, 17826.

52 R. A. Himes, G. Y. Park, G. S. Siluvai, N. J. Blackburn and K. D. Karlin, *Angew. Chem., Int. Ed.*, 2008, **47**, 9084.

53 D. P. Smith, D. G. Smith, C. C. Curtain, J. F. Boas, J. R. Pilbrow, G. D. Ciccotosto, T.-L. Lau, D. J. Tew, K. Perez, J. D. Wade, A. I. Bush, S. C. Drew, F. Separovic, C. L. Masters, R. Cappai and K. J. Barnham, *J. Biol. Chem.*, 2006, **281**, 15145.

